Decidua-derived Mesenchymal Stem Cells as carriers of Mesoporous Silica Nanoparticles. *In vitro* and *in vivo* evaluation on mammary tumors.

Juan L. Paris[1,2], Paz de la Torre[3], Miguel Manzano[1,2], M. Victoria Cabañas[1], Ana I. Flores[3*] and María Vallet-Regí[1,2*]

[1]Dpto. Química Inorgánica y Bioinorgánica, Facultad de Farmacia, UCM, Instituto de Investigación Sanitaria Hospital 12 de Octubre i+12, Madrid, Spain.

[2]CIBER de Bioingeniería, Biomateriales y Nanomedicina (CIBER-BBN).

[3]Grupo de Medicina Regenerativa, Instituto de Investigación Hospital 12 de Octubre i+12, Madrid, Spain.

[*]Corresponding authors: email: anaisabel.flores@salud.madrid.org; phone: 34 913908762 ; fax: 34 913908544; email: vallet@ucm.es; phone: 34 913941843; fax: 34 913941786

Keywords.

Nanoparticles, mesoporous silica; nanomedicine, human decidua-derived mesenchymal stem cells.

Abstract.

The potential use of human Decidua-derived mesenchymal stem cells (DMSCs) as a platform to carry mesoporous silica nanoparticles in cancer therapy has been investigated. Two types of nanoparticles were evaluated. The nanoparticles showed negligible toxicity to the cells, a fast uptake and a long

retention inside them. Nanoparticle location in the cell was studied by colocalization with the lysosomes. Moreover, the *in vitro* and *in vivo* migration of DMSCs towards tumors was not modified by the evaluated nanoparticles. Finally, DMSCs transporting doxorubicin-loaded nanoparticles were capable of inducing cancer cell death *in vitro*.

1. Introduction

The use of nanotechnology for drug delivery is nowadays changing the fields of biotechnology and biomedicine, allowing the incorporation of multiple therapeutic, sensing and targeting agents into nanoparticles (NPs).[1,2] Those NPs can be manufactured with a great variety of compositions and/or structures.[3] Among the different types of NPs, mesoporous silica NPs offer superior structural properties compared to other NPs, such as, large surface area and pore volume, tunable pore sizes, colloidal stability and robustness that allows straightforward functionalization of the silica walls.[4–6] NPs have been widely investigated as carriers for targeted drug delivery to cancer cells because they can overcome several inconveniences of systemic drug administration, such as poor solubility and limited stability of several drugs and side-effects due to non-specific uptake of the cytotoxic drugs by healthy cells.[7–9] In this sense, a key aspect of this technology is that NPs can be targeted and delivered into the tumors, which can be achieved by either passive targeting, through the enhanced permeability and retention (EPR) effect,[10,11] or active targeting, through the functionalization of nanoparticle surface with certain affinity ligands that would be specifically recognized by the targeted diseased cells.[12] However, the recent progress in nanotechnology has not

achieved the expected results in improving drug targeting,[13,14] highlighting the need of a better localization of the nanoparticles towards the tumor sites.

Human mesenchymal stem cells (MSCs), which are multipontent progenitors cells that maintain and regenerate connective tissues,[15] present migratory properties towards tumors. Those inherent tumor tropism and migratory properties suggest their possible use as carriers of NPs to isolated tumors and metastasic diseases.[16,17] A particular type of MSCs, those from the decidua of human placenta, have shown migratory capacity towards tumors *in vitro*, as well as in a preclinical model of breast tumors.[18] Although the driving force for DMSCs to migrate into tumor sites is unknown, it is already well known that human MSCs have high tropism towards tumors.[19] The inflammatory tumor microenvironment enables human MSCs to specifically home to tumor tissues. Several factors such as cytokines, growth factors, receptors, extracellular matrix and inflammation factors appear to be involved in this migration capacity.[20,21] More interestingly, DMSCs have been observed to inhibit the growth of primary tumors and the development of new tumors[18]. These observations, together with the facts that DMSCs are easy to obtain and constitute a homogeneous population, inspired the idea of using them as therapeutic agents and as cellular vehicles of nanoparticles towards tumors.

The aim of the present work is to exploit the benefits of the chemistry and biology of both systems. On one hand, NPs can be loaded with different chemical molecules and their surface can be easily modified with diverse chemical groups. On the other hand, the biological abilities of DMSCs, including the migration features towards tumors and the inherent inhibition of the growth of certain tumors, motivated the use of those cells as carriers of NPs towards

tumor cells. Although the idea of introducing NPs in MSCs has been already reported for actively targeted delivery,[22] this article investigates for the first time whether human DMSCs could be employed as a platform to load NPs and carry them to tumors for future anticancer therapies.

DMSCs, like other MSCs, are adult stem cells without the ethical concerns of embryonic cells, they present a low risk of viral infection and have low or non-immune response, and also show genomic stability under extended culture periods. Further, DMSCs present additional advantages respect to other MSCs sources, such us, the cells are easy to obtain, in a greater number and without invasive procedures. Moreover, the capacities of proliferation and differentiation of MSCs from other sources such as bone marrow or adipose tissue, are variable and dependent of the donor age while DMSCs present a high proliferantion and differentiation capacity. All these characteristics of DMSCs suggest that they could be considered a good and safe product for future clinical applications.

This work explores the internalization of two different types of NPs into DMSCs, the cellular retention capacity of the NPs, their effect on DMSCs survival and, the *in vitro* and *in vivo* migration capacity towards mammary tumor tissue. Also, the capacity of DMSCs carrying drug-loaded NPs to induce cancer cell death was evaluated. The integration of NPs with DMSCs would allow the design of a multifunctional platform for effective treatment of diseases such as cancer.

2. Experimental Section.

2.1 Fabrication and characterization of dye-doped NPs.

NPs were synthesized by modifying previous methods.[23] Briefly, APTES-dyes were synthesized by labeling 3-aminopropyl triethoxysilane (APTES) with active groups of dyes. For example, APTES (2.2 µL) was labeled with 1 mg of fluorescein isothiocyanate (FITC) in 100 µL of ethanol solution. The reaction mixture was stirred at room temperature for 2 h. Separately, cetyl-trimethylammonium bromide (CTAB) (1 g) was dissolved in 480 mL of deionized water and 3.5 mL of 2M NaOH were added with magnetic stirring. The mixture was heated to 80 ºC and left for 30 min. Then, 5 mL of tetraethyl orthosilicate (TEOS) for negatively-charged NPs (neg-NPs), or a mixture of TEOS and APTES (4.5 and 0.5 mL, respectively), for positively-charged NPs (pos-NPs), was added slowly during 20 min, then the particles were left at 80 ºC under stirring for 2 h. The resulting particles were collected by centrifugation and then washed three times with deionized water and ethanol, respectively. The surfactant template was removed by ion exchange using an extracting solution of NH_4NO_3 (10 mg/mL) in EtOH (95 %). The particles were suspended in that medium and magnetically stirred at 75 ºC overnight. The particles were centrifuged and washed three times with deionized water and ethanol. Surfactant removal was confirmed by thermogravimetric analysis.

All the reagents used for the synthesis of NPs were commercial products (Sigma-Aldrich, Spain) and were used without further purification.

The materials were analyzed by X-ray diffraction (XRD) in a Philips X-Pert MPD diffractometer equipped with Cu Kα radiation. Thermogravimetry and Differential Temperature Analysis (TGA/DTA) were performed in a Perkin Elmer Pyris Diamond TG/DTA analyser, with 5^{o}C/min heating ramps, from room temperature to 600ºC. Fourier Transformed Infrared (FTIR) spectra were

obtained in a Nicolet (Thermo Fisher Scientific) Nexus spectrometer equipped with a Smart Golden Gate Attenuated Total Reflectance (ATR) accessory. Surface morphology was analysed by Scanning Electron Microscopy (SEM) in a JEOL 6400 Electron microscope. Transmission Electron Microscopy (TEM) was carried out with a JEOL JEM 2100 instrument operated at 200 kV, equipped with a CCD camera (KeenView Camera). N_2 adsorption was carried out on a Micromeritics ASAP 2010 instrument; surface area was obtained by applying the Brunauer, Emmet &Teller (BET) method to the isotherm and the pore size distribution was determined by the Barrett, Joyner & Halenda (BJH) method from the desorption branch of the isotherm. The mesopore size was determined from the maximum of the pore size distribution curve. The Z-potential and hydrodynamic size of nanoparticles were measured in deionized water by means of a Zetasizer Nano ZS (Malvern Instruments) equipped with a 633 nm "red" laser.

2.2 Isolation and culture of DMSCs.

Human placentas from healthy mothers were obtained from the Department of Obstetrics and Gynecology under written informed consent approved by the Ethics Committee from *Hospital Universitario 12 de Octubre*. Processing of placental membranes and culture of primary cells was done as previously described.[18,24] Briefly, extra- embryonic membranes (amnion, chorion [fetal origin] and decidua [maternal origin]) were processed by enzymatic digestion with trypsin-EDTA (Lonza, Spain). Isolated cells were grown in Dulbecco's modified Eagle's medium (DMEM) supplemented with 2 mM of glutamine, 0.1 mM of sodium pyruvate, 55mM β-mercaptoethanol, 1 % non-essential amino acids, 1 % penicillin/streptomycin, 10 % fetal bovine serum and 10 ng/mL of

EGF (epidermal growth factor), at 37 ºC, 5 % CO_2 and 95 % humidity. Non-adherent cells were discarded after 5 days. In our preceding study, we reported the morphology, phenotype, maternal origin and MSCs characteristics of DMSCs.[24] At confluence, adherent cells were passaged and seeded at a density of 10^4 cells per cm^2.

2.3 Cellular uptake of particles by DMSCs.

DMSCs were plated 24 h before the start of the experiment in culture multiwell plates at a density of 10^4 cells per cm^2. After incubation with 200 µg/mL particles for 2 h, the media were replaced by fresh media and cells were incubated for one additional hour. The cells were fixed with Z-fix solution (Anatech, USA) for 15 min, permeabilized with 0.1 % Triton X-100 in phosphate buffer saline (PBS) solution, at room temperature, for 5 min and, subsequently incubated for 20 min with Alexa Fluor®568 phalloidin (Invitrogen, Spain) for staining F-actin. DAPI (40,60 diamidino-2-phenylindole) at 1 µg/mL was used to stain and visualize the nuclei. Fluorescence microscopy was performed with an Evos® FL Cell Imaging System equipped with tree Led Lights Cubes (lEX (nm); lEM (nm)): DAPI (357/44; 447/60), GFP (470/22; 525/50), RFP (531/40; 593/40) from AMG (Advance Microscopy Group). Quantitative analysis of cellular uptake was performed by flow cytometry (FACS). 200 µg/mL particles were incubated with the DMSCs for the indicated time points, and then removed by washing three times and cells were incubated for one additional hour. Subsequently, the cells were trypsinised, collected by centrifugation and redispersed in PBS solution with trypan blue (0.5 %) to remove extracellular fluorescence. The fluorescence intensity of 10,000 cells was quantified by FACS. Statistical analysis for differences between groups was carried out by the Student´s t test.

Quantitative analysis of retention ability of particles was performed by FACS. Particles at a concentration of 200 μg/mL were incubated with the MSCs for 2 h, and then removed by washing three times. The cells were then cultured in fresh medium for indicated time points. Subsequently, the cells were collected by trypsinization and centrifugation, and redispersed in PBS solution with trypan blue (0.5 %). The fluorescence intensity of 10,000 cells was quantified by FACS. The fluorescence intensities obtained after the first day were corrected by the cell dilution folds due to cell division.

2.4 Intracellular fate of NPs.

For the co-localization of NPs and lysosomes, the cells were incubated with 200 μg/mL particles for 2 h. The cells were washed twice with PBS solution. Then, lysosomes were stained with the Cell Tracker® Lysosome staining kit following the manufacturer protocol (AAT Bioquest, Inc, USA). The cells were washed twice with PBS, and then fresh medium was added. The cells were fixed and stained with DAPI as previously described. Fluorescence microscopy was performed with an Evos® FL Cell Imaging System.

2.5 Cytotoxicity of NPs.

The cytotoxicity of NPs was evaluated using the following standard protocols:

Lactate dehydrogenase (LDH) activity test: Extracellular LDH activity was measured in the media using the kit for Quantitative determination of LDH (Spinreact, Spain). DMSCs were incubated with NPs for 24 h at different concentrations. Then, the culture medium was collected for measuring the extracellular LDH activity. The LDH activity was directly measured by spectrophotometer at 340 nm in the culture medium following the manufacturer protocol.

MTS (3-(4,5-dimethylthiazol-2-yl)-5-(3-carboxymethoxyphenyl)-2-(4-sulfophenyl)-2H-tetrazolium) assay: The MTS reduction assay was performed using a commercial assay and following the manufacturer´s protocol (CellTiter® Aqueous One Solution Cell Proliferation Assay). Briefly, DMSCs were incubated with various concentrations of NPs for 2 h (n=3). The medium was replaced with 600 µL culture medium including MTS, and the incubation proceeded for 3 h. The medium was then removed, and its absorption at 490 nm was measured using a microplate reader.

2.6 Tissue homogenates from NMU-induced mammary tumors.

N-nitroso-N-methylurea (NMU) tumors were induced in 45-day-old Sprague-Dawley female rats according to our previously published protocol.[25] Concisely, NMU (Sigma-Aldrich, Spain) was administered once a week during two weeks by intra-peritoneal injection at a concentration of 5 mg/100g rat body weight. As well, metoclopramide (0.125 mg/L) was administered in the drinking water. Animals were palpated weekly for the detection of mammary tumors. The tumors were disected out from the animals, immediately frozen in liquid nitrogen and subsequently stored at -80 ºC until use.

Homogenates were performed at 4 ºC as we previously described.[18] The protein concentration was measured using the Lowry protein assay kit (Biorad, Spain) following the manufacturer´s instructions.

2.7 Transwell assay.

The *in vitro* effect of mammary tumor homogenate on DMSCs migration capacity was determined using Millicell culture plate inserts with 8 µm pore polycarbonate membranes (Merk Millipore, Spain) in 24-well plates. Briefly, $1.5x10^5$ DMSCs in 300 µL of serum-free DMEM were seeded in the insert.

Tumor homogenate (5 mg/mL of protein concentration was added in the well below. Migration medium (serum-free DMEM) without tissue was used as a negative control. Migration was assessed at 24 h by the CytoSelect 24-Well Cell Migration Assay (8 μm, Colorimetric, Cell Biolabs, Bionova Cientifica, S.L., Spain). Non-migratory cells were removed from the top of the membrane and migratory cells on the bottom of the polycarbonate membrane were stained with the Cell Stain Solution and quantified according to manufacturer´s instructions. Migratory cells were visualized (three individual fields per insert) using a light microscope under x40 magnification objective. Color of stained cells was subsequently extracted with the Extraction Solution, and quantified by absorbance at 560 nm using the multimodal plate reader Enspire (Perkin Elmer). All experiments were done as a minimum in triplicate.

2.8 *In vivo* migration.

To evaluate the *in vivo* migration capacity of NP loaded DMSCs, cells were incubated with pos-NPs as previously described. After washing non-internalized NPs, 10^6 cells were injected into the circulation through the tail-vein of Spraw-Dawley rats with NMU-mammary tumors. Seventy-two hours later, rats were anesthetized, and mammary tumors were removed and stored at -80ºC until use. Frozen tissue was sectioned in the cryostat, treated with Sudan Black to removed self-fluorescence following the manufacturer´s instructions, the nuclei were stained with DAPI for 1 min and sections were mounted with Vectashield and the tissue sections were visualized by fluorescence microscopy.

2.9 *In vitro* experiments with doxorubicin-loaded NPs

Doxorubicin was loaded in neg- and pos-NPs by stirring 10 mg of NPs in 5 mL of a 1 mg/mL solution of doxorubicin in PBS for 24 h. Doxorubicin-loaded NPs

(DOX-NPs) were washed by centrifugation and redispersion in PBS several times.

DMSCs were incubated with 200 μg/mL DOX-NPs for 2 h and washed with PBS to remove non-internalized nanoparticles. Cell viability was evaluated after 2 h, 1 day and 2 days by Alamar Blue assay, following the manufacturer´s instructions. Briefly, 10 % of the reagent was added to the culture medium with the DMSCs and incubated at 37 ºC for 1 h. Then, fluorescence at 560EX nm/590EM nm was measured in a microplate reader. Cell viability was then analyzed as a percentage of the control wells (DMSCs not exposed to DOX-NPs).

In order to determine the feasibility of using DOX-NPs inside DMSCs as a platform for future anticancer therapies, DMSCs with DOX-pos-NPs were co-cultured with NMU rat mammary cancer cells (ATCC, LGC Standards S.L.U., Spain). NMU cells were cultured in 24 well plates at a density of 20,000 cells per well. Twenty four hours later, three wells were trypsinized and cells were counted. Then, DMSCs with DOX-pos-NPs (incubated as described previously) were seeded in Transwell® culture inserts (0.4 μm pore, polycarbonate membranes, tissue cultured treated, Costar®) in two different DMSCs:NMU ratios (1:2 and 1:5). After 4 days, the inserts were removed and NMU cells were trypsinized and stained with BD Pharmingen™ FITC Annexin V Apoptosis Detection Kit I, following the manufacturer´s instructions. Then, the cells were analyzed by FACS. Statistical analysis was peformed by the Student´s t test.

3. Results and Discussion.

In order to evaluate DMSCs as potential carriers of NPs, mesoporous silica NPs (neg-NPs and pos-NPs) were synthesized according to a modified Stöber method [23]. Both types of NPs were covalently labeled with fluorescein by co-condensation during nanoparticle synthesis in order to be able to follow the fate of the NPs in contact with cells by fluorescence microscopy. Regarding particle morphology, SEM micrographs showed NPs, neg-NPs and pos-NPs, with spherical shape. Additionally, well-ordered mesoporous channels could be appreciated in the corresponding TEM micrographs (Figure 1). In fact, typical XRD patterns of MCM-41 type materials were observed in all cases, with the three characteristic maxima (*100*), (*110*) and (*200*), confirming the 2D hexagonal order of the mesopores arrangement (Figure S1). N_2 adsorption isotherms observed in all cases were type IV, with typical surface areas (1051 and 1109 m^2/g) and pore diameter (2.8 and 2.5 nm) for this type of negatively and positively-charged NPs, respectively. The NPs show a hydrodynamic particle diameter of *ca.* 190 nm. The charge of the NPs was confirmed through Z-potential (-31.5mV and +23.3mV, respectively), and the organic functionality through FTIR spectroscopy (Si-OH and $–NH_2$ groups, respectively) (Figure S1).

With respect to the interaction of the particles with the cells, in addition to size and shape, the NP surface is also a very important feature. The mechanism of NP internalization into the cell is generally via endocytosis,[26] a process in which extracellular materials are intracellularly incorporated into a membranous vesicle. The chemical groups attached to the surface of the NPs strongly influence their interaction with biological entities and, therefore, their internalization. In this sense, the surface of NPs can be easily modified through a functionalization process with a great variety of organic groups.[27] In an

effort to evaluate the contribution of surface chemistry, the effect of both charge and functionality on the cellular uptake, neg-NPs and pos-NPs was tested.

First, we incubated NPs with DMSCs to evaluate the toxicity of the nanoparticles on these cells in culture. Both negatively and positively-charged NPs were dispersed in serum-free medium at different concentrations and incubated with DMSCs for 2 h. Then, the nanoparticles were withdrawn and the cells were cultured in complete medium for 24 h. Cell viability was examined by LDH release and MTS reduction assay (Figure 2).

We observed that there was no increase in LDH released in the culture medium of DMSCs incubated with the NPs. This indicates that, at 24 h, the NPs did not induce cell death in DMSCs. Furthermore we looked to confirm these results using an assay that estimates the number of viable cells. The results of the MTS reduction assay (Figure 2) show that NPs did not induce significant toxicity over a very wide range of NP concentrations (at least up to 1 mg/mL). This is of great value for subsequent experiments because it is very important to have as much NPs as possible incorporated into cells.

Once toxicity was found not to be an issue, the next step was to evaluate the endocytosis process, studying how long the NPs remain inside the cells (retention time) and describing their location within the cells, whether lysosomal or cytoplasmic. To evaluate the endocytosis process, both types of NPs (negatively and positively-charged) were dispersed in serum-free DMEM and incubated with DMSCs for different periods of time. The concentrations of NPs, 100 and 200 µg/mL, were selected to avoid nanoparticle aggregates outside the cells (Figure S2). The NP suspension was then withdrawn and the cells were rinsed three times with PBS. Fluorescence microscopy images of DMSCs

incubated with neg-NPs and pos-NPs can be seen in Figure 3a. After staining cytoplasmatic actin with AlexaFluor®568 Phalloidin (red) and nuclei with DAPI (blue), NPs with a fluorescent dye attached are observed internalized into the cytoplasm of the DMSCs, with most cells carrying NPs when incubated at 200 µg/mL. The morphology of the cells remained unmodified after NP internalization (Figure S3).

When incubating NPs (green) with a concentration of 100 µg/mL, pos-NPs were observed to be internalized more efficiently than neg-NPs. The same trend was observed with higher concentrations (200 µg/mL). Thus, we found that 200 µg/mL and 2 h were the optimal concentration and incubation time parameters for the best internalization results. Besides, pos-NPs were internalized better in DMSCs than neg-NPs, with many particles localized around the nucleus after 2 h of incubation (Figure 3a).

The uptake of NPs was quantified using flow cytometry at different times of internalization (Figure 3b). The cells were dispersed in trypan blue solution in order to remove extracellular fluorescence and quantify only internalized nanoparticles. The results showed that, at shorter periods of time, the amount of endocytosed NPs was higher for those negatively charged, probably due to an electrostatic interaction of the positively-charged particles with the cell surface, delaying their internalization. However, after two hours, both types of NPs were effectively endocytosed, with percentages of cells with internalized NPs close to 85 % in all cases (Figure S4).

Fluorescence intensity of internalized particles followed the same trend, with more neg-NPs internalized after 1 h than pos-NPs (Figure 3b). However, after 2 h of incubation, the intensity of the pos-NPs was higher than the neg-NPs,

which indicates that the former NPs are better internalized than the later. All of these results are in agreement with previous results in the literature,[28] and could be explained by the stronger interaction of pos-NPs with negatively-charged phospholipids in the cell membrane. In order to check that interaction, the same cells dispersed in PBS were analyzed by flow-cytometry and intracellular and membrane-adhered NPs were measured. The fluorescence of membrane-adhered NPs was estimated as the difference of cell fluorescence in PBS and cell fluorescence in trypan blue solution. This extracellular fluorescence was 2.5 times higher for pos-NPs than for neg-NPs (data not shown). In any case, the necessary time to complete the internalization process was found to be 2 h, so this was the incubation time of NPs with cells for the subsequent experiments.

Once the NPs have been internalized, the next important parameter to consider is the retention time of the particles in the cells. According to previous studies by our group [18], it was found that 3 days is the necessary time for the DMSCs to reach the tumor tissues in an *in vivo* model, so the particles should remain in the cells a minimum of 3 days. The procedure to evaluate the retention capacity of the particles in DMSCs was similar to the uptake experiment, that is, cells were incubated with 200 µg/mL of both neg- and pos-NPs for 2 h, then washed and cultured for up to 5 days. Figure 3c shows the normalized fluorescence intensity percentage of the cells at different culturing times, being almost constant for the neg-NPs, which means that those NPs were retained in the cytoplasm. Pos-NPs fluorescence was kept unchanged at the initial stages, but after 1 day the intensity increased up to *ca.* 140 %. This could be explained by a slow uptake of membrane-adhered nanoparticles due

to interactions between pos-NPs and negatively-charged phospholipids at the cell membrane.[28] This means that in terms of retention capacity, a greater amount of particles were observed in the group of pos-NPs than in the neg-NPs. Most importantly, in all cases, NPs were still retained in the cells at day 5. Taking into account that it takes around 3 days for the cells to reach the tumor in the *in vivo* model previously evaluated,[18] those results guarantee that our NPs will be still in the cells when reaching the tumor tissue, validating our initial hypothesis of using DMSCs as carriers of nanoparticles.

Once internalization and retention of NPs into living mesenchymal cells were validated, the next step was exploring the location of internalized NPs in the cells. NPs are normally transported to the endo-lysosomal system after internalization, and the ability of the NPs to escape from the lysosomes is an important parameter regarding the stability of the NPs.[17]

A co-localization study was performed in DMSCs with internalized NPs by staining the cell lysosomes (Cell Navigator® Lysosome staining kit) and comparing the location within the cells of lysosomal red fluorescence and NP-associated green fluorescence. We observed that NPs were located inside lysosomes just after internalization (Figure S5), independently of their surface charge. However, after 3 days, the location of NPs inside the cells was different for pos-NPs and neg-NPs (Figure 3d). In neg-NPs, the fluorescence due to NPs was co-localized within the lysosomes, which indicates that neg-NPs were not able to escape the lysosomes in that time. On the other hand, fluorescence from pos-NPs does not match the fluorescence of the cell lysosomes at day 3, which shows that these NPs had escaped the lysosomes, probably by a charge-dependent mechanism previously described in the literature.[17] This result

indicates that pos-NPs could be a better option to be transported by DMSCs, as the lysosomal escape would ensure a less aggressive environment both for the NPs and its cargo.

All the above results show the stability of NPs in DMSCs, which is a necessary requirement to combine both elements. The internalization of the NPs into the cells and their persistence has been shown so far, so we next evaluated the migration capacity of NP-loaded DMSCs towards tumors. The *in vitro* and *in vivo* migrating capability of DMSCs towards tumors has been previously observed by our research group.[18] Here we evaluated if DMSCs with uptaken NPs retained those tumor tropism properties in an *in vitro* migration study. Thus, their *in vitro* migration capability was analyzed in the presence and absence of tumor human breast homogeneate using a standardized transwell migration assay (Figure 4). DMSCs without particles (control) and with both types of NPs were tested.

Compared to the migration in the absence of tumor homogenate, DMSCs migration capacity was almost 4 times higher when the tumor homogenate was present. Interestingly, the presence of any of the types of NPs (pos- and neg-) in the cells, did not appreciably affect the migration capacity of DMSCs toward tumor homogenate. Thus, combining these migration results together with cellular uptake, retention time and lysosomal leakage, it is clear that pos-NPs inside DMSCs is the best combination for the design of an efficient construct for drug delivery technologies. Therefore, pos-NPs were chosen to study the *in vivo* migration of DMSCs towards mammary tumors. DMSCs were cultured with pos-NPs and injected into the tail vein of NMU-induced tumor rats. After 3 days, the tumors were surgically removed, and the presence of green-fluorescent NPs was examined by fluorescence

microscopy. The results presented in Figure 5 show the presence of NPs inside the tumors, located around of some nuclei in the tissue. This indicates that the DMSCs retain their *in vivo* homing capacity towards the tumors when carrying NPs. These results show the ability of the cells to transport the NPs to the diseased site.

Regarding the antitumor application of this platform, NPs were loaded with doxorubicin, an anticancer drug. DOX-NPs were then incubated with DMSCs and cell viability was evaluated by Alamar Blue assay at different time points (Figure S6). DOX-neg-NPs induced significantly higher toxicity in DMSCs than DOX-pos-NPs after 2 days. This effect could be due to the higher doxorubicin loading capacity of neg-NPs previously reported in the literature,[29] which leads to higher toxicity. As a consequence, DOX-pos-NPs were chosen for the subsequent experiments.

The therapeutic potential of this approach was evaluated through an *in vitro* co-culture assay, using DMSCs with DOX-pos-NPs and NMU mammary cancer cells. DMSCs with or without drug-loaded NPs were seeded in the Transwell culture insert and the insert placed on top of a well that contains the NMU cells. Two different DMSC:NMU ratios (1:2 and 1:5) were tested. After 4 days, the Transwell inserts were removed and the NMU cells were evaluated by FACS using an apoptosis/necrosis detection kit (BD Pharmingen™ FITC Annexin V Apoptosis Detection Kit I). The Figure 6 shows that a significant fraction of the cancer cells became apoptotic/necrotic (cells appear in the right quadrants of the dot plots FL1-H *vs* FL2-H) only when the DMSCs were carrying DOX-NPs. Furthermore, this effect also appears to be dose-dependent, observing lower

cancer cell viability when larger amounts of DMSCs transporting DOX-NPs were present.

4. Conclusions.

Mesoporous silica nanoparticles (NPs) show negligible toxicity after being incubated with human Decidua-derived mesenchymal stem cells (DMSCs). NP uptake by DMSCs is fast (2 h) and the particles are retained inside the cells for a long period of time (at least 5 days), more than enough for DMSCs to accumulate in the tumor environment. The presence of NPs inside DMSCs does not inhibit their tumor-tropic behavior *in vitro* and *in vivo.* DMSCs transporting doxorubicin-loaded NPs were capable of inducing cell death in NMU cancer cells when co-cultured *in* vitro. All of these results indicate that DMSCs could be a promising platform for cancer therapy as carriers of anticancer drug-loaded NPs.

Acknowledgments.

Financial support from *Ministerio de Economía y Competitividad*, Spain (Project MAT2012-35556 and Project CSO2010-11384-E, Ageing Network of Excellence) and CIBER-BBN are gratefully acknowledged. CIBER-BBN is an initiative funded by the VI National R&D&i Plan 2008-2011, *Iniciativa Ingenio* 2010, Consolider Program, CIBER Actions and financed by the *Instituto de Salud Carlos III* with assistance from the European Regional Development Fund. The XRD measurements were performed at *C.A.I Difracción de Rayos X*, *Universidad Complutense de Madrid* (Spain). SEM and TEM were performed at ICTS National Centre for Electron Microscopy (Spain). JL Paris gratefully

acknowledges *Ministerio de Economía y Competitividad*, Spain, for his PhD grant (BES-2013-064182). This work was sponsored by grants from *Acción Estratégica en Salud* (FIS PI080137; PI11/00581); the MMA Foundation (FMMA 2008-108), and the Neurosciences and Aging Foundation, the *Francisco Soria Melguizo* Foundation, Octopharma and Parkinson Madrid (PI2012/0032). The authors are very grateful to M. Grau and D. de la Fuente for their assistance in the *in vivo* experiments.

Supplementary data*.* Full characterization of MSNs, Fluorescence microscopy images of DMSCs incubated with different concentrations of NPs, Percentage of DMSCs with internalized NPs by flow cytometry, colocalization of NPs and lysosomes at 0 days, cell viability % of DMSCs incubated with DOX-NPs after different periods of time.

References.

[1] O.C. Farokhzad, R. Langer, Impact of nanotechnology on drug delivery, ACS Nano. 3 (2009) 16–20.
[2] C. Minelli, S.B. Lowe, M.M. Stevens, Engineering nanocomposite materials for cancer therapy., Small. 6 (2010) 2336–2357.
[3] S.D. Steichen, M. Caldorera-Moore, N.A. Peppas, A review of current nanoparticle and targeting moieties for the delivery of cancer therapeutics., Eur. J. Pharm. Sci. 48 (2013) 416–27.
[4] C. Argyo, V. Weiss, C. Bräuchle, T. Bein, Multifunctional Mesoporous Silica Nanoparticles as a Universal Platform for Drug Delivery, Chem. Mater. 26 (2014) 435–451.
[5] M. Manzano, M. Colilla, M. Vallet-Regí, Drug delivery from ordered mesoporous matrices., Expert Opin. Drug Deliv. 6 (2009) 1383–400.
[6] M. Manzano, M. Vallet-Regí, New developments in ordered mesoporous materials for drug delivery, J. Mater. Chem. 20 (2010) 5593.
[7] J. Lu, M. Liong, J.I. Zink, F. Tamanoi, Mesoporous silica nanoparticles as a delivery system for hydrophobic anticancer drugs., Small. 3 (2007) 1341–1346.
[8] Z. Li, J.C. Barnes, A. Bosoy, J.F. Stoddart, J.I. Zink, Mesoporous silica nanoparticles in biomedical applications., Chem. Soc. Rev. 41 (2012) 2590–605.
[9] J. Lu, M. Liong, Z. Li, J.I. Zink, F. Tamanoi, Biocompatibility, biodistribution, and drug-delivery efficiency of mesoporous silica nanoparticles for cancer therapy in animals., Small. 6 (2010) 1794–805.

[10] J. Fang, H. Nakamura, H. Maeda, The EPR effect: Unique features of tumor blood vessels for drug delivery, factors involved, and limitations and augmentation of the effect., Adv. Drug Deliv. Rev. 63 (2011) 136–51.
[11] H. Maeda, H. Nakamura, J. Fang, The EPR effect for macromolecular drug delivery to solid tumors: Improvement of tumor uptake, lowering of systemic toxicity, and distinct tumor imaging in vivo, Adv. Drug Deliv. Rev. 65 (2013) 71–79.
[12] N. Bertrand, J. Wu, X. Xu, N. Kamaly, O.C. Farokhzad, Cancer nanotechnology: the impact of passive and active targeting in the era of modern cancer biology., Adv. Drug Deliv. Rev. 66 (2014) 2–25.
[13] I.K. Kwon, S.C. Lee, B. Han, K. Park, Analysis on the current status of targeted drug delivery to tumors., J. Control. Release. 164 (2012) 108–14.
[14] V.J. Venditto, F.C. Szoka, Cancer nanomedicines: so many papers and so few drugs!, Adv. Drug Deliv. Rev. 65 (2013) 80–8.
[15] M.F. Pittenger, A.M. Mackay, S.C. Beck, R.K. Jaiswal, R. Douglas, J.D. Mosca, et al., Multilineage potential of adult human mesenchymal stem cells., Science. 284 (1999) 143–147.
[16] Y.-L. Hu, Y.-H. Fu, Y. Tabata, J.-Q. Gao, Mesenchymal stem cells: a promising targeted-delivery vehicle in cancer gene therapy., J. Control. Release. 147 (2010) 154–62.
[17] Z. Gao, L. Zhang, J. Hu, Y. Sun, Mesenchymal stem cells: A potential targeted-delivery vehicle for anti-cancer drug, loaded nanoparticles, Nanomedicine Nanotechnology, Biol. Med. 9 (2013) 174–184.
[18] I. Vegh, M. Grau, M. Gracia, J. Grande, P. de la Torre, A I. Flores, Decidua mesenchymal stem cells migrated toward mammary tumors in vitro and in vivo affecting tumor growth and tumor development, Cancer Gene Ther. 20 (2013) 8–16.
[19] S. Kidd, E. Spaeth, J.L. Dembinski, M. Dietrich, K. Watson, A. Klopp, et al., Direct evidence of mesenchymal stem cell tropism for tumor and wounding microenvironments using in vivo bioluminescent imaging., Stem Cells. 27 (2009) 2614–23.
[20] E. Spaeth, A. Klopp, J. Dembinski, M. Andreeff, F. Marini, Inflammation and tumor microenvironments: defining the migratory itinerary of mesenchymal stem cells., Gene Ther. 15 (2008) 730–8.
[21] D. Bexell, S. Scheding, J. Bengzon, Toward brain tumor gene therapy using multipotent mesenchymal stromal cell vectors., Mol. Ther. 18 (2010) 1067–75.
[22] X. Huang, F. Zhang, H. Wang, G. Niu, K.Y. Choi, M. Swierczewska, et al., Mesenchymal stem cell-based cell engineering with multifunctional mesoporous silica nanoparticles for tumor delivery, Biomaterials. 34 (2013) 1772–1780.
[23] A. Baeza, E. Guisasola, A. Torres-Pardo, J.M. González-Calbet, G.J. Melen, M. Ramirez, et al., Hybrid enzyme-polymeric capsules/mesoporous silica nanodevice for in situ cytotoxic agent generation, Adv. Funct. Mater. 24 (2014) 4625–4633.
[24] M.I. Macias, J. Grande, A. Moreno, I. Domínguez, R. Bornstein, A.I. Flores, Isolation and characterization of true mesenchymal stem cells derived from human term decidua capable of multilineage differentiation into all 3 embryonic layers., Am. J. Obstet. Gynecol. 203 (2010) 495.e9–

495.e23.
[25] I. Vegh, R.E. de Salamanca, Prolactin, TNF alpha and nitric oxide expression in nitroso-N-methylurea-induced-mammary tumours., J. Carcinog. 6 (2007) 18.
[26] J.L. Vivero-Escoto, I.I. Slowing, B.G. Trewyn, V.S.-Y. Lin, Mesoporous silica nanoparticles for intracellular controlled drug delivery., Small. 6 (2010) 1952–67.
[27] F. Hoffmann, M. Cornelius, J. Morell, M. Fröba, Silica-based mesoporous organic-inorganic hybrid materials., Angew. Chem. Int. Ed. Engl. 45 (2006) 3216–51.
[28] T. Yu, A. Malugin, H. Ghandehari, Impact of silica nanoparticle design on cellular toxicity and hemolytic activity, in: ACS Nano, 2011: pp. 5717–5728.
[29] H. Meng, M. Xue, T. Xia, Y.-L. Zhao, F. Tamanoi, J.F. Stoddart, et al., Autonomous in Vitro Anticancer Drug Release from Mesoporous Silica Nanoparticles by pH-Sensitive Nanovalves, J. Am. Chem. Soc. 132 (2010) 12690–12697.

Figure Captions.

Figure 1. TEM (a, b) and SEM (c, d) micrographs of neg-NPs (left) and pos-NPs (right).

Figure 2. LDH release by DMSCs with internalized neg-NPs (blue)and pos-NPs (red) for 24 h(left); Cytotoxicity assay measured by MTS reduction of neg-NPs (blue)and pos-NPs (red) in DMSCs at 24 h after endocytosis (right). No significant differences were found at any of the evaluated concentrations (Data presented as Mean ± SD, N=3).

Figure 3. Fluorescence images of NP-loaded DMSCs; blue (nucleus), red (cytoplasm), green (NPs) (a), Flow-cytometry data regarding neg-NPs (blue) and pos-NPs (red) uptake (b) and retention (c) (Mean ± SD, N=3, *$p < 0.05$) , Colocalization study of NPs (green), nucleus (blue) and lysosomes (red) in DMSCs after 3 days (d).

Figure 4. *In vitro* Transwell migration assay of DMSCs against culture medium (basal), tumor homogenate (control) and migration of NP-loaded DMSCs against tumor homogenate. (Mean ± SD, N=3, *p < 0.05)

Figure 5. Fluorescence microscopy images of sections of NMU-induced rat adenocarcinomas after *in vivo* migration of DMSCs (images were taken 72 h after tail-vein injection of 10^6 DMSCs). Bright field images (a,c) of the tumor sections and Fluorescence images (b,d) of the same sections showing blue fluorescence of cell nuclei stained with DAPI and green fluorescence of the pos-NPs, indicating the *in vivo* migration towards tumors of DMSCs carrying pos-NPs.

Figure 6. Flow cytometry results of NMU cells after co-culture in different ratios with DMSCs or with DMSCs with internalized doxorubicin-loaded pos-NPs (DMSCs-NPs). NMU population analyzed (a), Apoptosis/Necrosis evaluation of NMU cells showing viable cells (lower left quadrant), early apoptotic cells (lower right quadrant) and late apoptotic/necrotic cells (upper right quadrant) (b-f), Percentage of viable NMU cells after co-culture (g). (Mean ± SD, N=3, *p < 0.05, **p < 0.01).

Figure 1

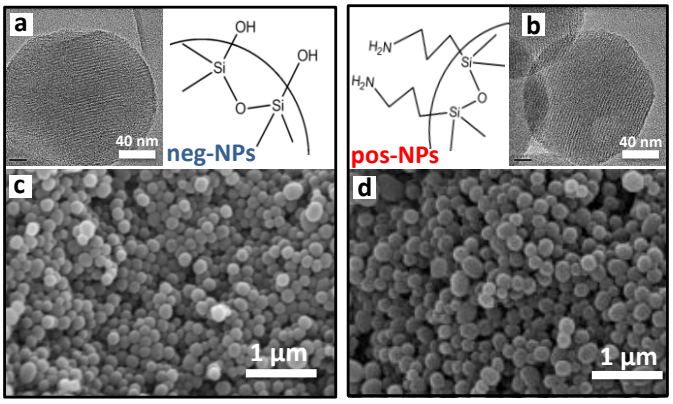

Figure 1.

Figure 2

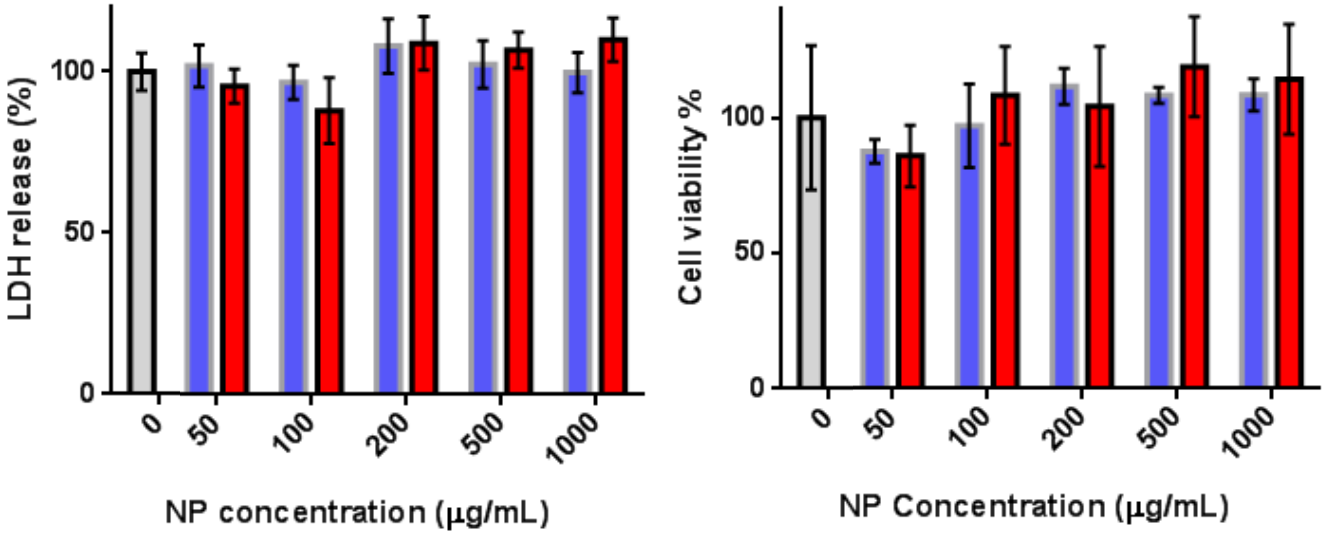

Figure 2.

Figure 3

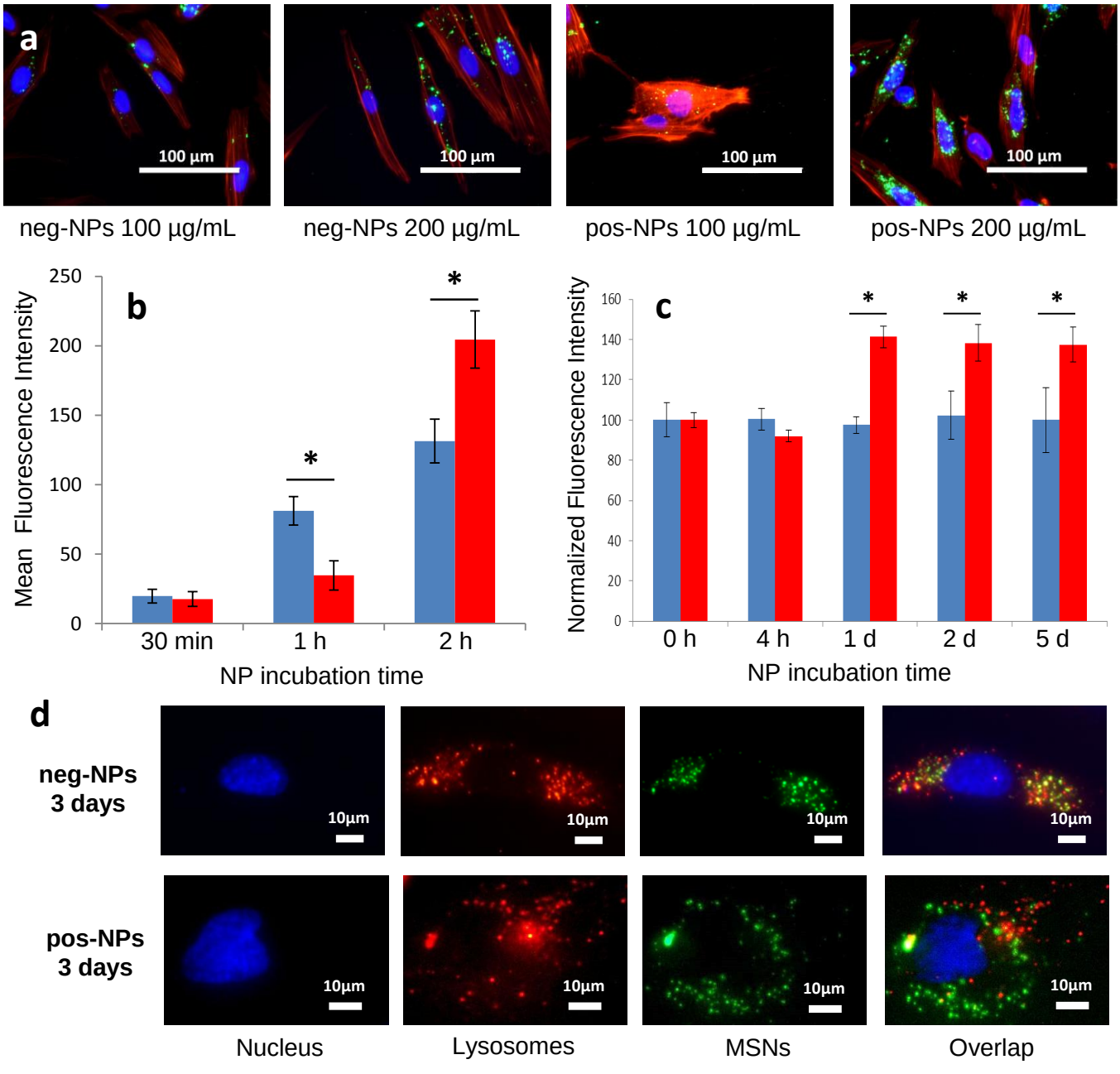

Figure 3.

Figure 4

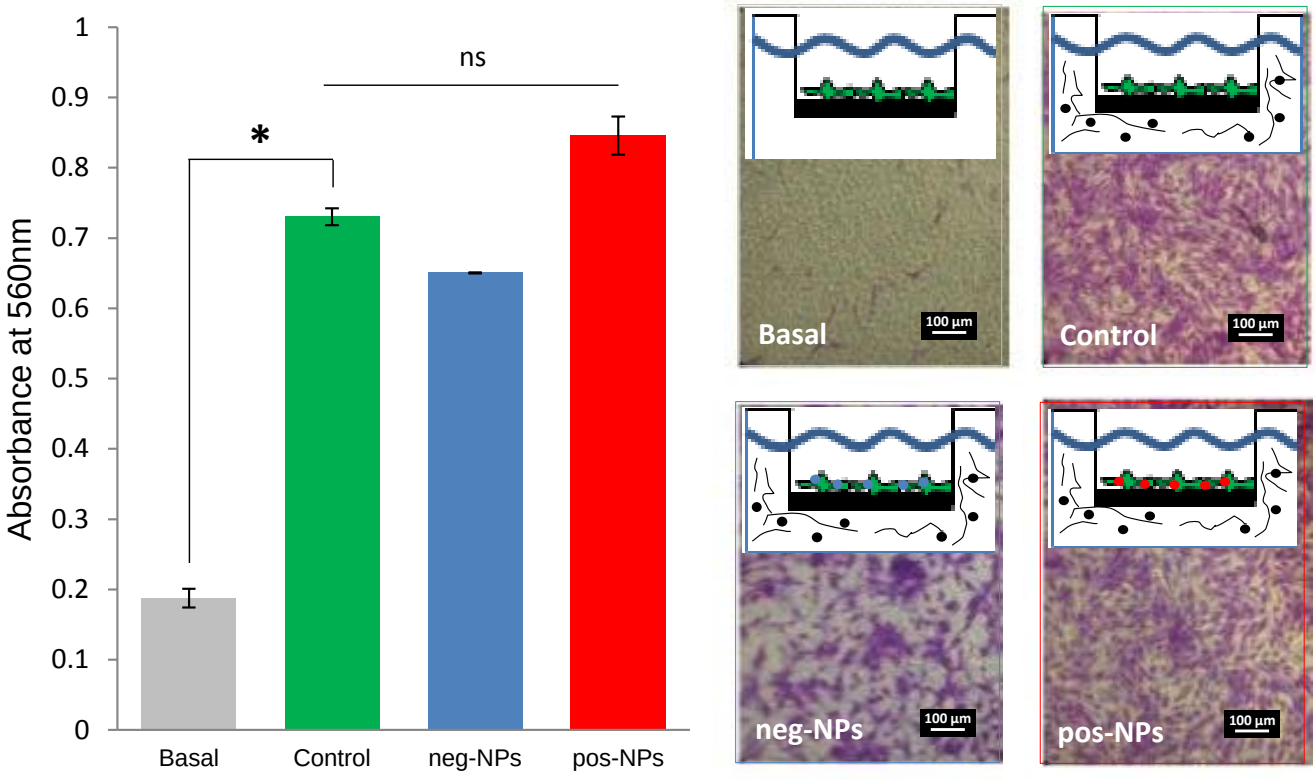

Figure 4.

Figure 5

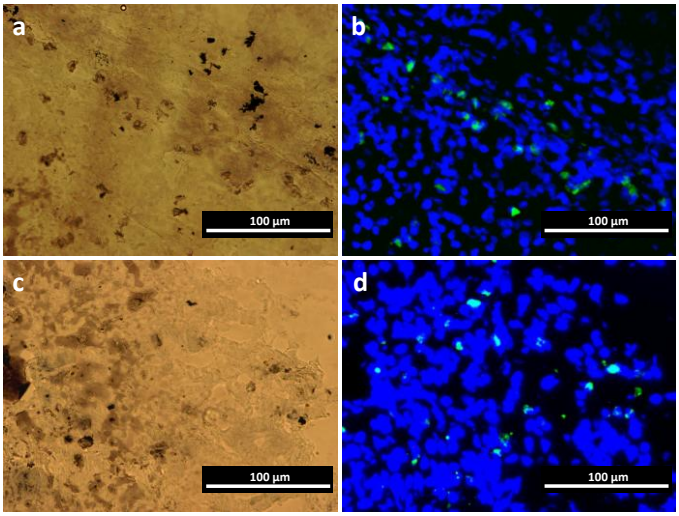

Figure 5.

Figure 6

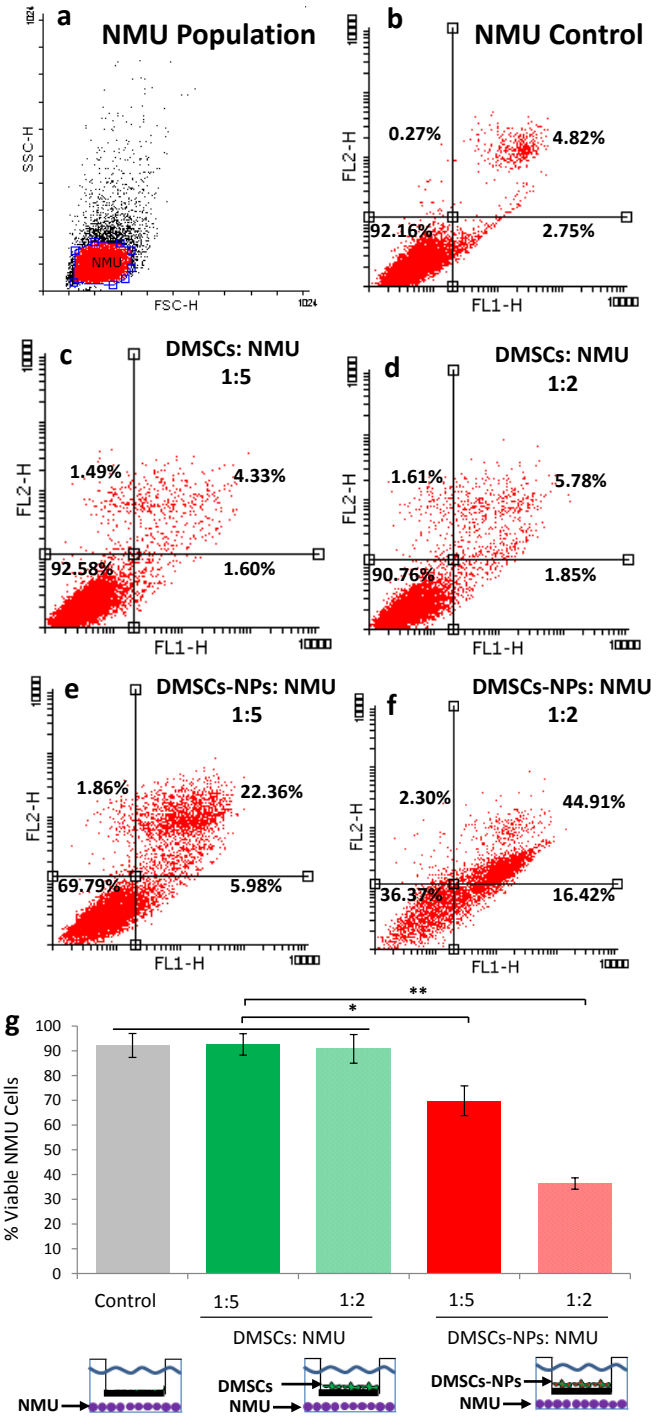

Figure 6.